Elastic and inelastic scattering of electrons from Ar and Cl

D.C. Griffin
Department of Physics, Rollins College, Winter Park, Florida 32789

M. S. Pindzola and T. W. Gorczyca
Department of Physics, Auburn University, Auburn, Alabama 36849

N. R. Badnell
Department of Physics and Applied Physics, University of Strathclyde, Glasgow, G4 0NG, United Kingdom
(Received 27 September 1994)

We have carried out extensive calculations of elastic and inelastic scattering of electrons from neutral argon and chlorine. The elastic and excitation cross sections are determined from the R-matrix method, in which the effects of dipole polarizability are included through the use of polarization pseudostates within the close-coupling expansions. For elastic scattering, our cross sections for Ar are compared to a number of other calculations and measurements. This provides a measure of the reliability of similar calculations for Cl. Our calculations of excitation include only transitions to the metastable levels of these atoms, where polarization effects are found to be quite important. Finally, ionization cross sections for these atoms are determined using the distorted-wave approximation; here, final-state correlation effects are found to be large.

PACS number(s): 34.80.Bm, 34.80.Dp

I. INTRODUCTION

Accurate calculations of electron scattering from complex neutral atoms and low-charge-state ions present a significant challenge to theoretical atomic physics. The effects of correlation within the target states of the atom or ion are often quite large, and coupling of the target states by the continuum electron can have large effects on the cross sections. In addition, polarization of the target by the continuum electron is difficult to represent accurately, and yet has a large effect on the size and shape of elastic and inelastic cross sections. Nevertheless, there is significant interest in calculations of electron scattering from such systems, primarily because of their applications to magnetically confined plasmas near the walls of fusion reactors, to plasma processing of microelectronic structures, and to low-temperature astrophysical plasmas.

There have been many measurements [1–6] and calculations [7–10] of elastic scattering from Ar, and comparison of any calculations with these results provides a measure of the accuracy of the theoretical methods employed. On the other hand, for elastic scattering from Cl, there is only one published calculation, which is at electron energies below 1.0 eV [11], and there are no measurements; this atom presents a somewhat greater theoretical challenge, because of the open $3p$ subshell.

There has been one calculation, using first-order many-body perturbation theory [12], and one R-matrix close-coupling calculation [13] of total excitation from the ground state to the metastable levels of Ar; however, no effort was made in these calculations to characterize the effects of polarization. In addition, there have been several measurements of excitation to the metastable levels in Ar, but there exist only a few experimental points for total cross section in the low-energy region. There have been no published calculations or measurements of excitation from the ground state to the metastable states of Cl. Finally, there have been many measurements (see, for example, Ref. [14]) and a number of calculations [15–17] for the ionization of Ar, but none for Cl.

In this paper, we present results for R-matrix close-coupling calculations of elastic scattering of electrons from neutral argon and chlorine, as well as electron-impact excitation to the lowest-lying metastable states of these atoms. We pay special attention to the effects of polarization of the core electrons on the scattering cross sections. In particular, we include polarization pseudostates within our close-coupling expansions in order to represent the effects of dipole polarizability on the scattering events. In addition, we employ the distorted-wave approximation to calculate the ionization cross sections for these atoms.

The remainder of this paper is arranged as follows. In the next section, we describe briefly the methods used to make these calculations. In Sec. III, we present our calculations for elastic scattering from Ar and Cl, and we make detailed comparisons of our results for Ar with other theoretical results and experimental data for this atom. In Sec. IV, we present our theoretical cross sections for excitation to the metastable states of Ar and Cl, using various levels of approximation. In Sec. V, we describe our distorted-wave results for ionization of Ar and Cl. Finally, in Sec. VI, we summarize our findings and discuss their implications.

II. COMPUTATIONAL METHODS

The R-matrix method provides an efficient means for solving the close-coupling equations. For this work, we

employed modified versions of the R-matrix programs, developed for the Opacity Project [18], to solve the scattering problem within the inner region. For the solutions in the asymptotic region, we employed the program FARM (Flexible Asymptotic R-Matrix package) developed by Burke and Noble [19]. It solves the scattering problem in the external region using a combination of R-matrix propagator techniques.

Fischer's multiconfiguration-Hartree-Fock (MCHF) programs [20] were employed to generate most of the bound-state radial wave functions. These codes allow for the generation of nonspectroscopic pseudo orbitals, that can be employed to represent core relaxation, term dependence, and configuration interaction within the target states.

In addition to the HF orbitals, we employed pseudo orbitals to allow for the polarization of the target by the scattering electron. Using a method introduced by Dalgarno and Lewis [21], the radial part of a pseudo orbital $P_{\bar{n}l'}(r)$, used to represent the polarization of a target electron with a radial wave function P_{nl}, can be determined, in the dipole approximation, by solving a differential equation of the form:

$$\left(-\frac{1}{2}\frac{d^2}{dr^2}-\frac{Z}{r}+\frac{l'(l'+1)}{2r^2}+V_{\rm HF}(r)-\epsilon_{nl}\right)P_{\bar{n}l'}(r)$$

$$=rP_{nl}(r)-\sum_{n_il_i}\delta_{l',l_i}\langle P_{nl}\,|r|\,P_{n_il_i}\rangle P_{n_il_i}(r). \qquad (1)$$

In this equation, $V_{\rm HF}$ is used to represent both the direct and exchange Hartree-Fock potential functions; in addition, we include projection operators within this function to force orthogonality with bound orbitals having the same angular momentum [22]. ϵ_{nl} is the eigenvalue of the Hartree-Fock equations for the target electron and the sum over n_il_i is over all bound electrons with the same angular momentum as the pseudo orbital.

These polarization pseudo orbitals are subsequently normalized and used to form a set of pseudostates that, when included in the close-coupling expansion, approximate the effects of polarization on the scattering event. The limitation of this method is based primarily on the number of such states that can be reasonably included within a close-coupling calculation. As we will see, for open-shell systems, the number of pseudostates needed to provide a proper representation of the effects of polarization can become quite large.

Polarization effects have also been incorporated in both bound and continuum calculations in atoms and low-charge-state ions through the use of various semiempirical polarization potentials. For example, a polarization potential of the form:

$$V_{\rm pol}=-\frac{\alpha}{2r^4}[1-\exp(-r^6/r_c^6)] \qquad (2)$$

was first introduced by Norcross and Seaton [23], where α is the dipole polarizability and r_c is a cutoff radius. It has been employed successfully for a number of bound-state and electron-impact excitation calculations involving one free electron above a closed shell (see for example, the calculations in Ca^+ by Mitroy *et al.* [24]). In addition, the potential first introduced by Baylis [25]:

$$V_{\rm pol}=-\frac{\alpha}{2}\frac{r^2}{(r^2+r_c^2)^3} \qquad (3)$$

has been applied by Brage *et al.* [26] to perform bound-state calculations in Ca I and Ca II. The use of either of these two polarization potentials for scattering calculations is much simpler than the extensive use of polarization pseudostates. For that reason, we have tested the use of Eq. (3) in the case of elastic scattering from Ar and employed it to represent the effects of polarization on the ionization cross section of both Ar and Cl.

The calculations of ionization cross sections were performed using our distorted-wave ionization cross section program [27]. This configuration-average ionization code has been modified to allow for ionization from a given LS term of the target atom to a particular LS term of the final ion. This program also allows for the inclusion of configuration interaction in the target states and the variation of the radial wave function for the ejected continuum electron with LS term (i.e., term dependence in the continuum).

The calculations of elastic and inelastic cross sections discussed in this paper were performed in LS coupling. For excitation of these atoms, an intermediate-coupling representation, using a Breit-Pauli Hamiltonian, would be more appropriate; this is especially true of Ar, where the excited states are best represented in j-K coupling. However, this would significantly complicate already complex calculations; furthermore, because we have restricted our excitation calculations to the $3p \rightarrow 4s$ transition to the metastable states of these atoms, the LS representation is still meaningful. We determine the cross section to particular metastable levels by multiplying the excitation cross section to the corresponding LS term by the appropriate statistical factor.

III. ELASTIC SCATTERING

A. Argon

There exists a large number of calculations and measurements of elastic scattering from neutral argon. Summaries of the more recent of these are given by Dasgupta and Bhatia [9] and by Saha [10]. The available data provide an opportunity to test the accuracy of theoretical methods, before making other calculations of electron scattering in this region of the periodic table.

We studied elastic scattering in Ar, using a restricted set of target states. Our primary motivation was to determine how well one could represent the scattering event with a single spectroscopic state and a small number of polarization pseudostates. As we shall see, restricting the calculation to a small number of states becomes particularly important for calculations of open-shell systems, such as Cl. Polarization of Ar occurs primarily within

the $3p$ subshell. Therefore, one should be able to represent most of the effects of polarization on elastic scattering by performing a close-coupling calculation, which includes only the ground state and those pseudostates which can be reached by a dipole excitation out of the $3p$ subshell.

Thus, we started our work on Ar by performing a two-state calculation, which included only $3p^6\ ^1S$ and $3p^5\bar{3}d\ ^1P$. The $1s$, $2s$, $2p$, $3s$, and $3p$ orbitals were determined from a single-configuration Hartree-Fock calculation on $3p^6\ ^1S$, while $P_{\bar{3}d}$, the radial part of the $\bar{3}d$ pseudo orbital, was determined by solving Eq. (1), with V_{HF} equal to the potential for a d orbital within a $p^5d\ ^1P$ term, and with $nl = 3p$. We found that we could obtain convergence in the scattering calculation for electron energies up to 20 eV by including partial waves from L=0 through L=4, where L is the total angular momentum of the atom plus free-electron system. The results for the total elastic cross section from this calculation agreed reasonably well with measurements and other calculations above about 5 eV. However, it did not show a Ramsauer minimum. Using this $3p^5\bar{3}d\ ^1P$ pseudostate, we also calculated the dipole polarizability of Ar, and obtained a value of 10.2 a_0^3, compared to the experimental value of $11.1a_0^3$ [28].

Next, we generated a $3p^5\bar{4}s\ ^1P$ polarization pseudostate (to complete the possible dipole excitations out of the $3p$ subshell) and performed a three-state calculation. This additional state had only a small effect on the total cross section above 5 eV, but significantly affected its shape below that energy; it then had a Ramsauer minimum close in shape and position to that obtained experimentally. However, with the addition of this $3p^5\bar{4}s^1P$ state, we calculated a dipole polarizability of $12.8a_0^3$. It is somewhat surprising that the low-energy portion of the cross section agrees well with experiment, when the value of the polarizability is about 15% above the experimental value.

Finally, we added a $3s3p^6\bar{4}p\ ^1P$ polarization pseudostate, corresponding to a dipole excitation out of the $3s$ subshell, and performed a four-state calculation. As one might expect, this had a very small effect on the size and shape of the cross section, as well as the value of the dipole polarizability. We show the results of our final four-state calculation for the total cross section, in comparison to other calculations and measurements, in Figs. 1 and 2. Over all, the comparison with these other data is quite good. From Fig. 1, we see that in the higher-energy region, our calculated cross section is somewhat low compared to the measurements; however, as mentioned by Dasgupta and Bhatia [9], this may be at least partially due to contributions of inelastic processes within the measured cross sections that should onset at about 11.6 eV. The agreement of our calculated cross section with the experimental measurements near the Ramsauer minimum is shown clearly in Fig. 2.

Our calculated cross section appears to be in the best agreement with the calculations of Dasgupta and Bhatia [9], who employed the polarized orbital method due to Temkin [29]. They used only a single $3p^5\bar{3}d\ ^1P$ pseudostate; however, their $\bar{3}d$ pseudo orbital was renormalized to give the experimental polarizability. Our results

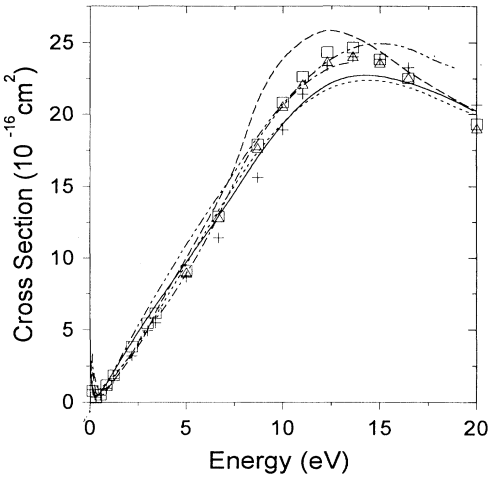

FIG. 1. Total cross section for elastic scattering from Ar. Solid curve, present 4-state R-matrix calculation; dashed curve, calculation of Saha [10]; dotted curve, calculation of Dasgupta and Bhatia [9]; dash-dot curve, calculation of Amusia [7]; dash-double-dot curve, calculation of Bell *et al.* [8]; open squares, measurements of Jost *et al.* [3]; plus signs, measurements of Ferch *et al.* [5]; open triangles, measurements of Nickel *et al.* [4].

are in good agreement with the calculations of Bell *et al.* [8] in the low-energy region, but are lower than their cross section in the higher-energy region. This is somewhat surprising, since their results are also based on R-matrix close-coupling calculations. However, they employed a single multiconfiguration ^1P pseudostate that was represented by a linear combination of $3p^5\bar{3}d$, $3p^5\bar{4}s$, and $3p^5\bar{4}d$ configurations using the method developed by Vo

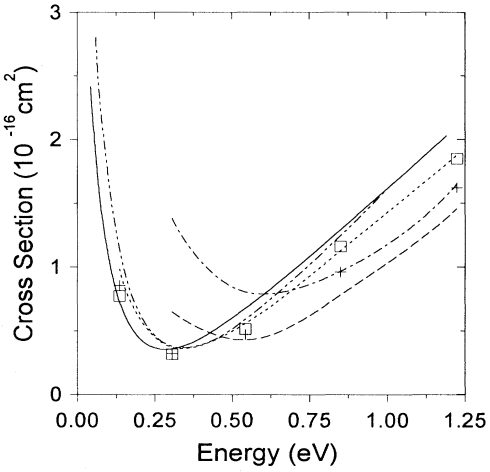

FIG. 2. Total cross section for elastic scattering from Ar in the region of the Ramsauer minimum. Solid curve, present 4-state R-matrix calculation; dashed curve, calculation of Saha [10]; dotted curve, calculation of Dasgupta and Bhatia [9]; dash-dot curve, calculation of Amusia [7]; dash-double-dot curve, calculation of Bell *et al.* [8]; open squares, measurements of Jost *et al.* [3]; plus signs, measurements of Ferch *et al.* [5].

Ky Lan *et al.* [30]. In Figs. 1 and 2, we notice some discrepancy with both the many-body perturbation theory calculations of Amusia *et al.* [7] and the more recent continuum multiconfiguration Hartree-Fock calculations of Saha [10]; however, the spread in the cross sections in the higher-energy region is only about 12% which appears acceptable in light of the simplicity of the present calculations.

In Fig. 3, we show our results for the momentum-transfer cross section for elastic scattering in Ar, in comparison to experimental measurements and other calculations. Our cross section is somewhat low compared to the other calculations, but the spread within the various theoretical calculations, near the peak in the cross section, is about the same as that within the experimental results.

Because of the simplicity of polarization potential methods compared to the extensive use of pseudostates, we also performed a calculation of the total elastic cross section in Ar, using the potential of Eq. (3) and a single $3p^6\ ^1S$ state. The results for the total elastic cross section from that calculation, in comparison to our four-state calculation, with four values of r_c from 1.0 to 2.0 are shown in Fig. 4. As can be seen, for $r_c = 2.0$, we obtain excellent agreement with our four-state calculation above about 5 eV. Because of the greater sensitivity of the calculation to the details of the scattering potential at low electron energies, the discrepancy is greater below 5 eV. A value of $r_c = 1.66$ (the average radius of the $3p$ orbital) may give the best overall results. There is a larger discrepancy in the higher-energy region; however, this is no greater than the spread between the various theoretical calculations shown in Fig. 1. Furthermore, the agreement with the four-state calculation is better below 5 eV. Nevertheless, it is disappointing that one does not see a Ramsauer minimum in the cross section

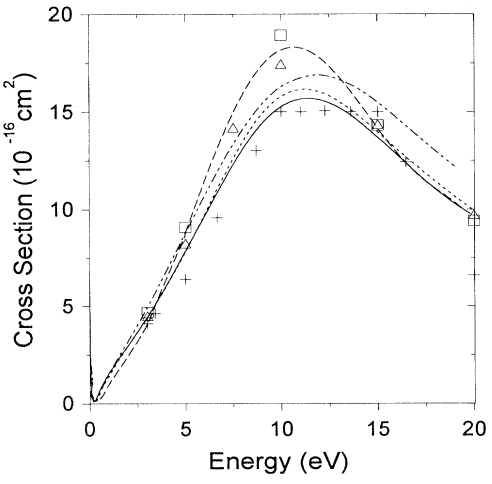

FIG. 3. Momentum-transfer cross section for elastic scattering from Ar. Solid curve, present 4-state R-matrix calculation; dashed curve, calculation of Saha [10]; dotted curve, calculation of Dasgupta and Bhatia [9]; dash-double-dot curve, calculation of Bell *et al.* [8]; open squares, measurements of Williams *et al.* [1]; plus signs, measurements of Srivastava *et al.* [2]; open triangles, measurements of Andrick [6].

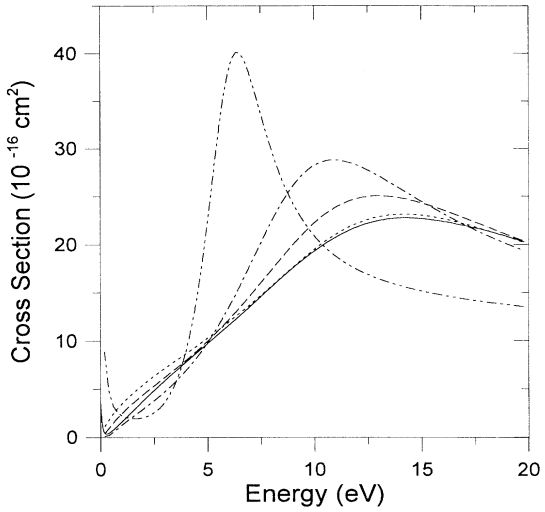

FIG. 4. Total cross section for elastic scattering from Ar. Solid curve, present 4-state R-matrix calculation. Other curves, single-state calculation using the Baylis polarization potential, Eq. (3), with $\alpha = 11.1$ and various cutoff radii: dotted curve, $r_c = 2.00$; dashed curve, $r_c = 1.66$; dash-dot curve, $r_c = 1.33$; dash-double-dot curve, $r_c = 1.00$.

until $r_c = 1.0$, and then the shape in the cross section is quite different from that obtained from the four-state calculation.

B. Chlorine

Based on the results obtained for elastic scattering in Ar, we have performed a similar calculation in Cl, using $\bar{3}d$, $\bar{4}s$, and $\bar{4}p$ polarization pseudo orbitals. However, because of the open $3p$ subshell in this atom, single-electron promotions out of the $3s$ and $3p$ subshells lead to many more states. In fact, a calculation comparable to the four-state calculation in Ar requires seventeen states in Cl. The terms employed in the Cl calculation are listed in Table I. For each value of L and S, the single-configuration terms listed for the sixteen even-parity states were then allowed to mix within a configuration-interaction calculation to form the final sixteen even-parity states included within the seventeen-state close-coupling expansion. Boyle [31] has recently developed an average potential for open-shell systems that includes all the first-order correlations in the diagrammatic series of the dipole polarizability. We employed this potential in Eq. (1) to determine the $\bar{3}d$ and $\bar{4}s$ pseudostates used to represent the effects of dipole excitations out of the $3p$ subshell. The effects of dipole excitations out of the 3s subshell are small, and by leaving out these promotions, the close-coupling calculation could have been reduced to ten states with very little loss in accuracy.

Again, partial waves up to $L = 4$, were sufficient to obtain convergence up to the maximum energy considered, which for Cl was 16.0 eV. The results of our calculation for the total and momentum-transfer cross sections for elastic scattering in Cl are shown in Fig. 5. The cross

TABLE I. The terms used for the 17-state calculation of elastic scattering in Cl.

$3s^23p^5\ ^2P^o$			
$3s3p^6\ ^2S^e$	$3s^23p^4(^1D)\bar{3}d\ ^2S^e$	$3s^23p^4(^1S)\bar{4}s^2S^e$	$3s3p^5(^3P)\bar{4}p\ ^2S^e$
$3s3p^5(^1P)\bar{4}p\ ^2S^e$	$3s^23p^4(^3P)\bar{3}d\ ^2P^e$	$3s^23p^4(^1D)\bar{3}d\ ^2P^e$	$3s^23p^4(^3P)\bar{4}s\ ^2P^e$
$3s3p^5(^3P)\bar{4}p\ ^2P^e$	$3s3p^5(^1P)\bar{4}p\ ^2P^e$	$3s^23p^4(^1S)\bar{3}d\ ^2D^e$	$3s^23p^4(^3P)\bar{3}d\ ^2D^e$
$3s^23p^4(^1D)\bar{3}d\ ^2D^e$	$3s^23p^4(^1D)\bar{4}s\ ^2D^e$	$3s3p^5(^3P)\bar{4}p\ ^2D^e$	$3s3p^5(^1P)\bar{4}p\ ^2D^e$

The $\bar{3}d$ pseudo orbital was determined from Eq. (1) using the average potential of Boyle [31].
The $\bar{4}s$ pseudo orbital was determined from Eq. (1) using the average potential of Boyle [31].
The $\bar{4}p$ pseudo orbital was determined from Eq. (1) for the $3s3p^5(^3P)\bar{4}p\ ^2D^e$ term.

sections are similar to our results for Ar, although the magnitude of the cross sections at the peaks is somewhat larger. The Ramsauer minimum is at a higher energy and is very well pronounced. On the basis of our comparisons in Ar, we would expect that the error in the magnitude of these cross sections would be at the ten to fifteen percent level.

The only published calculation of elastic scattering from Cl was performed very recently by Fabrikant [11] by the extrapolation of potential parameters along isoelectronic series and among corresponding neutral atoms. However, this calculation was restricted to energies below 0.6 eV. A comparison in the region of the Ramsauer minimum is difficult, since our minimum occurs at about 0.7 eV; however, it does appear that the minimum determined in Ref. [11] is somewhat lower in energy ($\sim$ 0.4 eV), and has a value of $\sim 3\times10^{-16}$ cm^2, compared to our minimum of $\sim 2.1\times10^{-16}$ cm^2.

In addition, Rescigno recently calculated elastic scattering from Cl using the complex Kohn variational principle [32]. The cross section from this calculation is similar to ours in the higher-energy region and has a Ramsauer minimum at approximately the same energy; however, the minimum is less pronounced and the cross section at the minimum is larger.

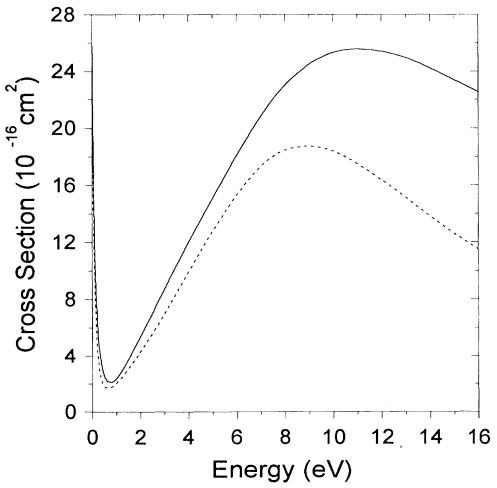

FIG. 5. 17-state R-matrix calculation of elastic scattering from Cl. Solid curve, total cross section; dotted curve, momentum-transfer cross section.

IV. ELECTRON-IMPACT EXCITATION

In this section, we consider electron-impact excitation to the lowest-lying metastable levels of Ar and Cl. We wish to study these excitations as a function of the number of states included within the close-coupling expansions, with special attention to the amount of polarization included in the calculations.

A. Argon

As mentioned earlier, there have been two previous calculations of excitation to the metastable states in Ar. One by Padial *et al.* [12], used first-order many-body perturbation theory; it is essentially a distorted-wave calculation in which the distorted waves are calculated in the potential of the ground state. The other calculation by Ojha *et al.* [13] was a nine-state R-matrix calculation, in which the core orbitals were determined from the Hartree-Fock solutions for the ground state of Ar^+ and the orbitals for excited states were optimized on various excited terms of neutral Ar. Neither of these calculations attempted to specifically incorporate the effects of polarization.

We began our work on excitation to the metastable states of Ar by carrying out both nine-state and sixteen-state calculations, without the inclusion of polarization pseudostates. The terms used in the close-coupling expansion for these calculations are listed within the first two parts of Table II. The $\bar{4}d$ pseudo orbital was generated from a MCHF calculation on $3p^53d\ ^1P + 3p^5\bar{4}d\ ^1P$ and corrects the $3d$ orbital, obtained from a configuration-average Hartree-Fock calculation, for the strong term dependence of this orbital within the $3p^53d\ ^1P$ term. Again, terms of the same LSII were allowed to mix within a configuration interaction calculation, before the close-coupling calculation was initiated. We also included configuration interaction of the ground state with $3p^43d^2\ ^1S$, $3p^44s^2\ ^1S$, and $3p^44p^2\ ^1S$. It is somewhat difficult to compare the calculated energies with experiment, since the experimental values are given in pair-coupling notation [33]. However, identification of the levels in LS coupling is possible for the $3p^54s$ and $3p^54p$ configurations, and at least the ^1P level of the $3p^53d$ configuration. A comparison for these levels with respect to the ground state indicates that the theoretical values are all high, with deviations varying from 0.25 eV to about

0.5 eV. In the case of the ^3P term, of primary interest here, the calculated energy is 12.0 eV compared to the experimental value of 11.6 eV [33].

As in the case of elastic scattering, inclusion of partial waves up to $L = 4$ was sufficient to obtain convergence in the excitation calculation. A comparison of the nine-state and sixteen-state calculations of the excitation cross section from the ground state to the $3p^5 4s\ ^3P_{0,2}$ metastable levels is shown in Fig. 6. The total cross sections to these two levels were determined by multiplying the calculated cross sections to $3p^5 4s\ ^3P$ by 0.667, the fraction of the statistical weights of these levels. As can be seen, continuum coupling with the terms of $3p^5 3d$ has a strong effect on excitation to $3p^5 4s\ ^3P$, reducing the cross section near the peak by more than a factor of two. However, the shape of the resonance structure in the lower-energy region is quite similar in the two calculations.

In this figure, we also show the few available measurements in this energy range. The measurements of Mason and Newell [34] were for total metastable production, including excitation to higher levels which cascade to the $^3P_{0,2}$ levels. Only their point at 12 eV is completely cascade free. The total cross sections of Chutjian and Cartwright [35] were determined by them from the integration of electron energy-loss measurements of the differential cross sections. However, the only measurements within this energy region were at 16 and 20 eV. Finally, Schappe *et al.* [36] have very recently reported measurements of excitation into the metastable states of Ar by the method of laser-induced fluorescence. The points shown in Fig. 6 were determined by adding the cross sections to the $^3P_0$ and $^3P_2$ levels from the curves given in their paper. We show the approximate uncertainty in their measurements at the peak of their cross section. Their curves do not show any sign of a resonance structure below 14 eV, but it is not clear from their pa-

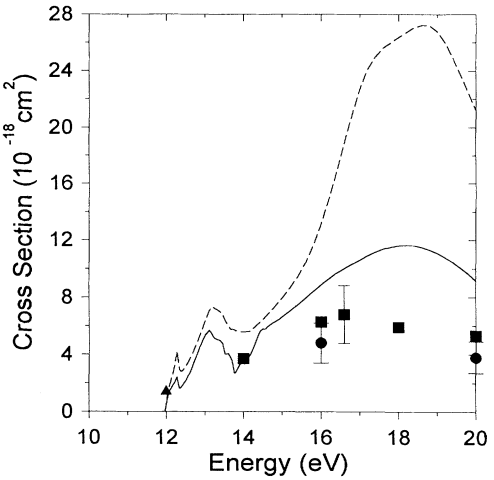

FIG. 6. Electron-impact excitation of Ar to the $3p^5 4s\ ^3P_{0,2}$ levels. Dashed curve, 9-state R-matrix calculation; solid curve, sixteen-state R-matrix calculation; solid triangle, measurement of Mason and Newell [34]; solid circles, measurements of Chutjian and Cartwright [35]; solid squares, from the measurements of Schappe *et al.* [36].

TABLE II. The terms used in the R-matrix calculations for Ar ($3p^6\ ^1S \rightarrow 3p^5 4s\ ^3P_{0,2}$).

(Configuration interaction with $3p^4 3d^2\ ^1S^e$, $3p^4 4s^2\ ^1S^e$, and $3p^4 4p^2\ ^1S^e$ is included.)			
1. 9-state R matrix			
$3p^6\ ^1S^e$	$3p^5 4s\ ^3P^o$	$3p^5 4s\ ^1P^o$	$3p^5 4p\ ^3S^e$
$3p^5 4p\ ^3D^e$	$3p^5 4p\ ^1D^e$	$3p^5 4p\ ^1P^e$	$3p^5 4p\ ^3P^e$
$3p^5 4p\ ^1S^e$			
The $1s$, $2s$, $2p$, $3s$, and $3p$ orbitals are from a HF calculation for $3p^6\ ^1S^e$.			
The $4s$ orbital is from a HF calculation for $3p^5 4s\ ^3P^o$.			
The $4p$ orbital is from a configuration-average HF calculation for $3p^5 4p$.			
2. 16-state R matrix			
9 terms above plus:			
$3p^5 3d\ ^3P^o$	$3p^5 3d\ ^3F^o$	$3p^5 3d\ ^1F^o$	$3p^5 3d\ ^1D^o$
$3p^5 3d\ ^3D^o$	$3p^5 3d\ ^1P^o$	$3p^5 \bar{4}d\ ^1P^o$	
The $3d$ orbital is from a configuration-average HF calculation for $3p^5 3d$.			
The $\bar{4}d$ pseudo orbital was determined from a MCHF calculation on $3p^5 3d\ ^1P + 3p^5 \bar{4}d\ ^1P$.			
3. 18-state R matrix			
16 terms above plus the polarization pseudostates:			
$3p^5 \bar{5}s\ ^1P^o$	$3p^5 \bar{5}d\ ^1P^o$		
The $\bar{5}s$ polarization pseudo orbital was determined from Eq. (1) for the $3p^5 \bar{5}s\ ^1P$ term.			
The $\bar{5}d$ polarization pseudo orbital was determined from Eq. (1) for $3p^5 \bar{5}d\ ^1P$ term.			
4. 33-state R matrix			
18 terms above plus the additional polarization pseudostates:			
$3p^4(^1S)4s(^2S)\bar{5}s\ ^3S^e$	$3p^4(^1D)4s(^2D)\bar{5}d\ ^3S^e$	$3p^5 \bar{5}p\ ^3S^e$	$3p^4(^3P)4s(^4P)\bar{5}s\ ^3P^e$
$3p^4(^3P)4s(^2P)\bar{5}s\ ^3P^e$	$3p^4(^3P)4s(^4P)\bar{5}d\ ^3P^e$	$3p^4(^3P)4s(^2P)\bar{5}d\ ^3P^e$	$3p^4(^1D)4s(^2D)\bar{5}d\ ^3P^e$
$3p^5 \bar{5}p\ ^3P^e$	$3p^4(^1D)4s(^2D)\bar{5}s\ ^3D^e$	$3p^4(^3P)4s(^4P)\bar{5}d\ ^3D^e$	$3p^4(^3P)4s(^2P)\bar{5}d\ ^3D^e$
$3p^4(^1S)4s(^2S)\bar{5}d\ ^3D^e$	$3p^4(^1D)4s(^2D)\bar{5}d\ ^3D^e$	$3p^5 \bar{5}p\ ^3D^e$	
The $\bar{5}p$ polarization pseudo orbital was determined from Eq. (1) for the $3p^5 \bar{5}p\ ^3S$ term.			

per how many measurements were actually made in this low-energy region.

Despite the small amount of experimental data available, it is clear that the nine-state calculation far overestimates the cross section. By adding more continuum coupling, we obtain significant improvement with regard to agreement with experiment; however, the sixteen-state calculation still appears to be well above the measurements.

It may be that the remaining discrepancy is due to polarization effects not already included in the sixteen-state calculation. However, it is important to note that with the $3p^5 4s\ ^1P^o$, $3p^5 3d\ ^1P^o$, and $3p^5 \bar{4}d\ ^1P^o$ terms, we have included some polarization of the ground state and with the $3p^5 4p\ ^3S^e$, $3p^5 4p\ ^3P^e$, $3p^5 4p\ ^3D^e$ terms, we have included some polarization of the $3p^5 4s\ ^3P^o$ term, even though the excited orbitals were not generated for this purpose. We examined this for polarization out of the ground state, by making a fourteen-state calculation, in which the $3p^5 3d\ ^1P^o$, and $3p^5 \bar{4}d\ ^1P^o$ terms were not included. The resulting cross section is significantly lower than that obtained using the nine-state calculation, having a peak at 18 eV of $\sim 16\times10^{-18}$ cm^2. Thus, more than two thirds of the continuum coupling, arising from the addition of the $3p^5 3d$ configuration to the close-coupling expansion, is not associated with the dipole polarizability of the ground state.

We now consider additional R-matrix calculations which attempt to include the most important effects due to polarization of the target. We first examined the polarization of the ground state by adding the two polarization pseudostates $3p^5 \bar{5}s\ ^1P^o$ and $3p^5 \bar{5}d\ ^1P^o$, formed by a dipole excitation of the $3p$ electron out of $3p^6\ ^1S$, to our close-coupling expansion. We ignored the states formed from excitation out of the $3s$ subshell, since they had such a small effect in the case of elastic scattering. The specifics regarding the pseudo orbitals are given in the third part of Table II. The results of this eighteen-state calculation are shown by the dashed curve in Fig. 7. By comparing this result to the sixteen-state calculation (dotted curve), we see that this additional polarization of the ground state has had a relatively small effect.

Finally, we considered the polarization pseudostates formed from dipole excitations out of the $3p$ and $4s$ subshells of $3p^5 4s\ ^3P^o$. This led to the fifteen additional terms listed in the fourth part of Table II. It is important to note that the $\bar{5}s$ and $\bar{5}d$ pseudo orbitals used within the states formed from excitation out of the $3p$ subshell of $3p^5 4s\ ^3P^o$ were generated for excitation out of the $3p$ subshell of $3p^6\ ^1S$. This will introduce some error into the calculation; it could be corrected, but would require the use of additional pseudo orbitals. The results of this 33-state calculation are shown by the solid curve in Fig. 7. We see that this final-state polarization has a large effect on the cross section. Above 14 eV, the cross section appears to be in better agreement with experiment and may be within the uncertainty of the most recent measurements by Schappe *et al.* [36]. However, the largest effect is on the resonance structure centered at about 13 eV. Whether or not this enhancement of the resonance is real will not be known until high-resolution measurements in the resonance region can be made.

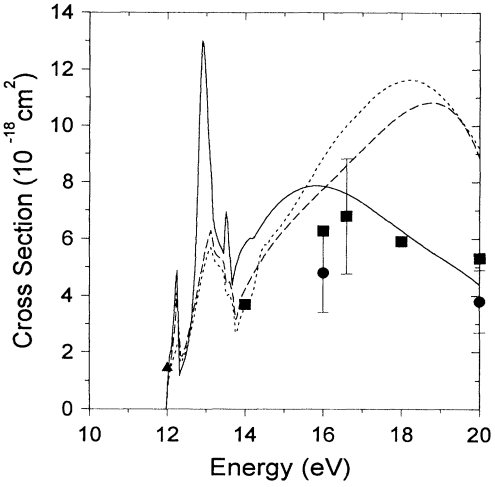

FIG. 7. Electron-impact excitation of Ar to the $3p^5 4s\ ^3P_{0,2}$ levels. Dotted curve, sixteen-state R-matrix calculation; dashed curve, 18-state R-matrix calculation; solid curve, 33-state R-matrix calculation; solid triangle, measurement of Mason and Newell [34]; solid circles, measurements of Chutjian and Cartwright [35]; solid squares, from the measurements of Schappe *et al.* [36].

It should be mentioned that by including these polarization pseudostates in the close-coupling expansion, we introduce pseudoresonances into the calculation. However, these are above the positions of the real resonances, and cause only small variations in the cross section within the energy range shown in Fig. 7. These were eliminated in Fig. 7, by smoothing the cross section in the energy range above the highest possible resonances attached to real states.

B. Chlorine

Since coupling of the $3p^5 4s\ ^3P$ metastable term to the terms of $3p^5 3d$ is found to be important in Ar, we began our work on Cl by performing a 29-state calculation, which included all the terms of the $3p^5$, $3p^4 4s$, $3p^4 4p$, $3p^4 3d$, and $3s3p^6$ configurations. The specific terms making up the close-coupling expansion for this calculation are listed in the first part of Table III. This corresponds to the 16-state calculation for Ar, with one exception: because of the presence of the $3s3p^6$ configuration in Cl, a $\bar{4}d$ pseudo orbital was generated from a MCHF calculation on $3s^2 3p^4(^1D)3d\ ^2S^e + 3s3p^6\ ^2S^e + 3s^2 3p^4(^1D)\bar{4}d\ ^2S^e$. The mixing between $3s^2 3p^4(^1D)3d\ ^2S^e$ and $3s3p^6\ ^2S^e$ is very strong, and is not properly represented by a configuration-interaction calculation with frozen orbitals; however, by including the $\bar{4}d$ pseudo orbital within a MCHF calculation, one can incorporate the relaxation in the radial orbital necessary to properly represent this mixing.

With respect to the ground state, most of the calculated terms are higher than the experimental energies [37], with deviations ranging from 0.04 eV to 0.78 eV;

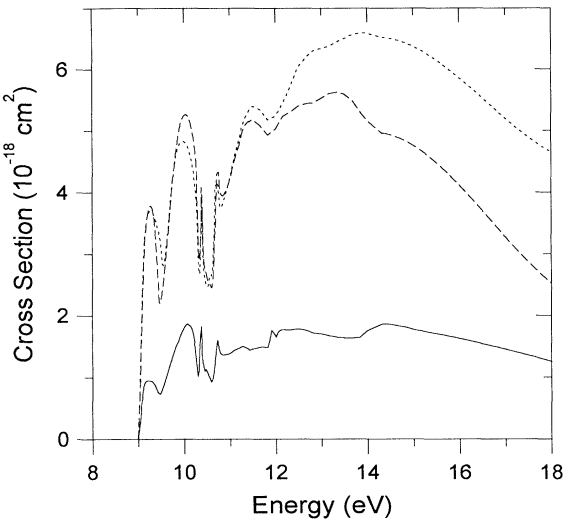

FIG. 8. Electron-impact excitation of Cl to the $3p^4 4s\ ^4P_{5/2}$ level. Dotted curve, 29-state R-matrix calculation; dashed curve, 37-state R-matrix calculation; solid curve, 51-state R-matrix calculation.

however, the great majority of calculated terms differ from the experimental values by less than 0.5 eV. In the case of the $3p^4(^3P)4s^4P$ metastable term, the calculated energy is 9.01 compared to the experimental value of 8.93 eV [37].

Again, inclusion of partial waves up to L=4 was sufficient to reach convergence in the excitation calculation for Cl. The 29-state calculation of the cross section for excitation from the ground state to the $3p^4(^3P)4s\ ^4P_{5/2}$ metastable level is shown by the dotted curve in Fig. 8. This cross section was determined by multiplying the cross section to $3p^4(^3P)4s\ ^4P$ by 0.5, the fraction of the statistical weights for this level.

As in the 16-state calculation in Ar, the 29-state calculation in Cl includes a limited amount of polarization; however, we attempted to incorporate additional polarization effects on the excitation cross section by performing calculations which include a set of polarized pseudostates within the close-coupling expansions. We began by adding those pseudostates which are formed from dipole excitations out of the $3p$ subshell of the $3p^5\ ^2P$ ground state. These are listed in the second part of Table III. Fortunately, we discovered that the strong mixing between $3s^2 3p^4(^1D)3d\ ^2S^e$ and $3s3p^6\ ^2S^e$ could be represented as well as was done with the $\bar{4}d$ pseudostate in the 29-state calculation by using the $3s^2 3p^4(^1D)\bar{4}d\ ^2S^e$ polarization pseudostate; this eliminated the necessity of including an additional set of states with a $\bar{5}d$ polarization pseudo orbital. The results of this 37-state calculation are shown by the dashed curve in Fig. 8. As can be seen, this additional polarization has an effect primarily above 12 eV and reduces the cross section by about 45

TABLE III. The terms used in the R-matrix calculations for Cl ($3p^5\ ^2P \rightarrow 3p^4 4s\ ^4P_{5/2}$).

(Configuration interaction with $3p^3 3d^2\ ^2P^o$, $3p^3 4s^2\ ^2P^o$, and $3p^3 4p^2\ ^2P^o$ is included.)

1. 29-state R-matrix calculation

$3p^5\ ^2P^o$	$3p^4(^3P)4s\ ^4P^e$	$3p^4(^3P)4s\ ^2P^e$	$3s3p^6\ ^2S^e$
$3p^4(^3P)4p\ ^4P^o$	$3p^4(^3P)4p\ ^4D^o$	$3p^4(^3P)4p\ ^2P^o$	$3p^4(^3P)4p\ ^2D^o$
$3p^4(^3P)4p\ ^4S^o$	$3p^4(^3P)4p\ ^2S^o$	$3p^4(^1D)4s\ ^2D^e$	$3p^4(^3P)3d\ ^4D^e$
$3p^4(^3P)3d\ ^4F^e$	$3p^4(^3P)3d\ ^4P^e$	$3p^4(^3P)3d\ ^2F^e$	$3p^4(^3P)3d\ ^2P^e$
$3p^4(^3P)3d\ ^2D^e$	$3p^4(^1D)3d\ ^2S^e$	$3p^4(^1D)4p\ ^2P^o$	$3p^4(^1D)4p\ ^2F^o$
$3p^4(^1D)4p\ ^2D^o$	$3p^4(^1D)3d\ ^2G^e$	$3p^4(^1D)3d\ ^2F^e$	$3p^4(^1D)3d\ ^2P^e$
$3p^4(^1D)3d\ ^2D^e$	$3p^4(^1S)4s\ ^2S^e$	$3p^4(^1S)3d\ ^2D^e$	$3p^4(^1S)4p\ ^2P^o$
$3p^4(^1D)\bar{4}d\ ^2S^e$			

The $1s$, $2s$, $2p$, $3s$, and $3p$ orbitals are from a HF calculation for $3p^5\ ^2P^o$.
The $4s$ orbital was determined from a HF calculation for $3p^4(^3P)4s\ ^4P^e$.
The $4p$ orbital was determined from a configuration-average HF calculation for $3p^4 4p$.
The $3d$ orbital was determined from a configuration-average HF calculation for $3p^4 3d$.
The $\bar{4}d$ pseudo orbital was generated from a $3p^4(^1D)3d\ ^2S^e + 3s3p^6\ ^2S^e + 3p^4(^1D)\bar{4}d\ ^2S^e$ MCHF calculation.

2. 37-state R matrix

The first 28 terms above [excluding $3p^4(^1D)\bar{4}d\ ^2S^e$] plus the polarization pseudostates:

$3p^4(^1S)\bar{5}s\ ^2S^e$	$3p^4(^1D)\bar{4}d\ ^2S^e$	$3p^4(^3P)\bar{5}s\ ^2P^e$	$3p^4(^3P)\bar{4}d\ ^2P^e$
$3p^4(^1D)\bar{4}d\ ^2P^e$	$3p^4(^1D)\bar{5}s\ ^2D^e$	$3p^4(^3P)\bar{4}d\ ^2D^e$	$3p^4(^1S)\bar{4}d\ ^2D^e$
$3p^4(^1D)\bar{4}d\ ^2D^e$			

The $\bar{5}s$ polarization pseudo orbital was determined from Eq. (1) for the $3p^4(^1D)\bar{5}s\ ^2D$.
The $\bar{4}d$ polarization pseudo orbital was determined from Eq. (1) for the $3p^4(^3P)\bar{4}d\ ^2D$.

3. 51-state R matrix

The 37 terms from above plus the additional polarization pseudostates:

$3p^3(^4S)4s(^5S)\bar{5}s\ ^4S^o$	$3p^3(^4S)4s(^3S)\bar{5}s\ ^4S^o$	$3p^3(^2D)4s(^3D)\bar{4}d\ ^4S^o$	$3p^4(^3P)\bar{5}p\ ^4S^o$
$3p^3(^2P)4s(^3P)\bar{5}s\ ^4P^o$	$3p^3(^2P)4s(^3P)\bar{4}d\ ^4P^o$	$3p^3(^2D)4s(^3D)\bar{4}d\ ^4P^o$	$3p^4(^3P)\bar{5}p\ ^4P^o$
$3p^3(^2D)4s(^3D)\bar{5}s\ ^4D^o$	$3p^3(^4S)4s(^5S)\bar{4}d\ ^4D^o$	$3p^3(^4S)4s(^3S)\bar{4}d\ ^4D^o$	$3p^3(^2P)4s(^3P)\bar{4}d\ ^4D^o$
$3p^3(^2D)4s(^3D)\bar{4}d\ ^4D^o$	$3p^4(^3P)\bar{5}p\ ^4D^o$		

The $\bar{5}p$ polarization pseudo orbital was determined from Eq. (1) for the $3p^4(^3P)\bar{5}p\ ^4P$.

percent at 18 eV.

Finally, we added those polarization pseudostates that are formed from dipole excitations out of the $3p$ and $4s$ subshells of $3p^4(^3P)4s\ ^4P$. These are listed in the last section in Table III. The results of this 51-state calculation are shown by the solid curve in Fig. 8. We see that final-state target polarization has a very large effect on the cross section, reducing the peak cross section at ~13.5 by about 70%. As in the case of Ar, the small effect due to pseudoresonances in the energy range of interest was eliminated in both the 37-state and the 51-state calculation by smoothing these cross sections above the highest possible resonances attached to real states.

V. ELECTRON-IMPACT IONIZATION

Finally, we consider electron-impact ionization of Ar and Cl. The configuration-resolved ionization method makes use of LS-term specific angular algebra, which is obtained from a modified version of the WEIGHTS program of Scott and Hibbert [38]. The method may include multiconfiguration approximations for the target atom and the resulting ion, with orbitals calculated using Fischer's MCHF program [20]. A prior form for the scattering amplitude is employed in which the initial and final scattered-electron wave functions are calculated in a V^N potential and the ejected-electron wave function is calculated in a V^{N-1} potential, where N is the number of bound electrons in the target atom [39,40]. For all initial and final scattered-electron wave functions, and most of the ejected-electron wave functions, the distorted-wave potential is a configuration-average Hartree potential for the direct interaction and a local semiclassical approximation for the exchange interaction [41]. For both Ar and Cl, the important dipole-allowed excitation contributions to the total ionization cross section include both ground-state and final-state correlations [15,27].

Ground-state correlations are incorporated through the use of multiconfiguration Hartree-Fock wave functions and the calculation of the additional terms in the scattering amplitude arising from the nonorthogonality of bound pseudostates and the continuum. Final-state correlations are included through the use of term-dependent Hartree-Fock wave functions for the ejected electron. For the photoionization of atoms, the appropriate term-dependent Hartree-Fock wave function is determined by choosing a potential for which all first-order final-state interactions sum to zero. For closed-shell atoms [42,43], this procedure produces a potential, which is equivalent to the potential found from a variation on the energy of the dipole-allowed continuum state. For open-shell atoms [44,31], this procedure produces a potential which is not equivalent, in general, to the potential found from a variation on the energy. In fact, for almost closed-shell atoms, like Cl, the appropriate Hartree-Fock potential, which includes all first-order final-state interactions, is quite different from the Hartree-Fock potential determined by energy variation. The appropriate potentials for photoionization, and for the dipole-allowed excitation contributions to electron ionization, are characterized by having large positive dipole exchange terms.

A. Argon

The electron-impact ionization cross section for the $3p^6\ ^1S \rightarrow 3p^5\ ^2P$ transition of Ar is shown in Fig. 9. Three distorted-wave calculations are presented. The first uses configuration-average potentials for all continuum orbitals. The second includes both ground-state and final-state correlations for the dipole-allowed $3p^6\ ^1S \rightarrow 3p^5(^2P)kd\ ^1P$ excitation contribution to the total ionization cross section. Ground-state correlations are included through a $3p^6$ and $3p^4\bar{3}d^2$ multiconfiguration Hartree-Fock calculation. Final-state correlations are included by calculating the kd ejected wave in a frozen-core term-dependent Hartree-Fock potential given by

$$V(^2P\ kd\ ^1P) = V_{\rm CA}({\rm core}) + 5J^0_{3p} - \frac{1}{5}J^2_{3p} + \frac{14}{15}K^1_{3p} - \frac{9}{35}K^3_{3p}\ , \qquad (4)$$

where $V_{\rm CA}({\rm core})$ is a configuration-average Hartree-Fock potential for the core electrons, J^λ_{3p} are direct terms, and K^λ_{3p} are exchange terms. The large repulsive exchange term in Eq. (4) reduces the overlap between the bound $3p$ orbital and the kd ejected wave, causing a large reduction in the ionization cross section. The effects of polarization are included in the third distorted-wave calculation by adding the polarization potential of Eq. (3) (with $r_c = \bar{r}_{3p}$) to the scattering potential for all continuum orbitals.

The total ionization cross section measurements of Wetzel *et al.* [14] are also shown in Fig. 9. The comparison between theory and experiment is valid since the $3s$ subshell ionization cross section is much smaller

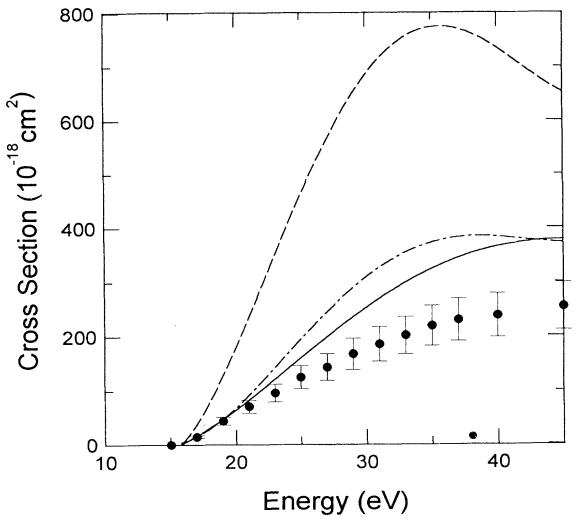

FIG. 9. Electron-impact ionization cross section for the $3p^6\ ^1S \rightarrow 3p^5\ ^2P$ transition in Ar. Dashed curve, distorted-wave calculation with configuration-average continuum orbitals; Solid curve, distorted-wave calculation including both ground- and final-state correlations for the dipole-allowed excitation contribution; Chained curve, distorted-wave calculation including correlations and a polarization potential. Solid circles, experimental measurements of Wetzel *et al.* [14] for the total cross section of Ar.

than the $3p$ subshell cross section. The first and second distorted-wave calculations compare well with the previous distorted-wave results of Younger [15] and the distorted-wave–R-matrix hybrid results of Bartschat and Burke [16]. The recent coupled-channel-optical calculations of McCarthy and Zhou [17] are lower than the distorted-wave calculations and, thus, are in much better agreement with experiment.

B. Chlorine

The electron-impact ionization cross sections for the $3p^5\ ^2P \rightarrow 3p^4(^3P,^1D,^1S)$ transitions in Cl are shown in Fig. 10. Three distorted-wave calculations are presented for each final LS term of the resulting ion. The first uses configuration-average potentials for all continuum orbitals. The second includes both ground-state and final-state correlations for the dipole-allowed $3p^5\ ^2P \rightarrow 3p^4(^3P)kd\ ^2(D,P)$; $3p^5\ ^2P \rightarrow 3p^4(^1D)kd\ ^2(D,P,S)$; and $3p^5\ ^2P \rightarrow 3p^4(^1S)kd\ ^2D$ excitation contributions to the total ionization cross section. Ground-state correlations are included through a $3p^5$ and $3p^3\bar{3}d^2$ multiconfiguration Hartree-Fock calculation. Final-state correlations are included by calculating the kd ejected waves in various frozen-core term-dependent Hartree-Fock potentials [44] given by

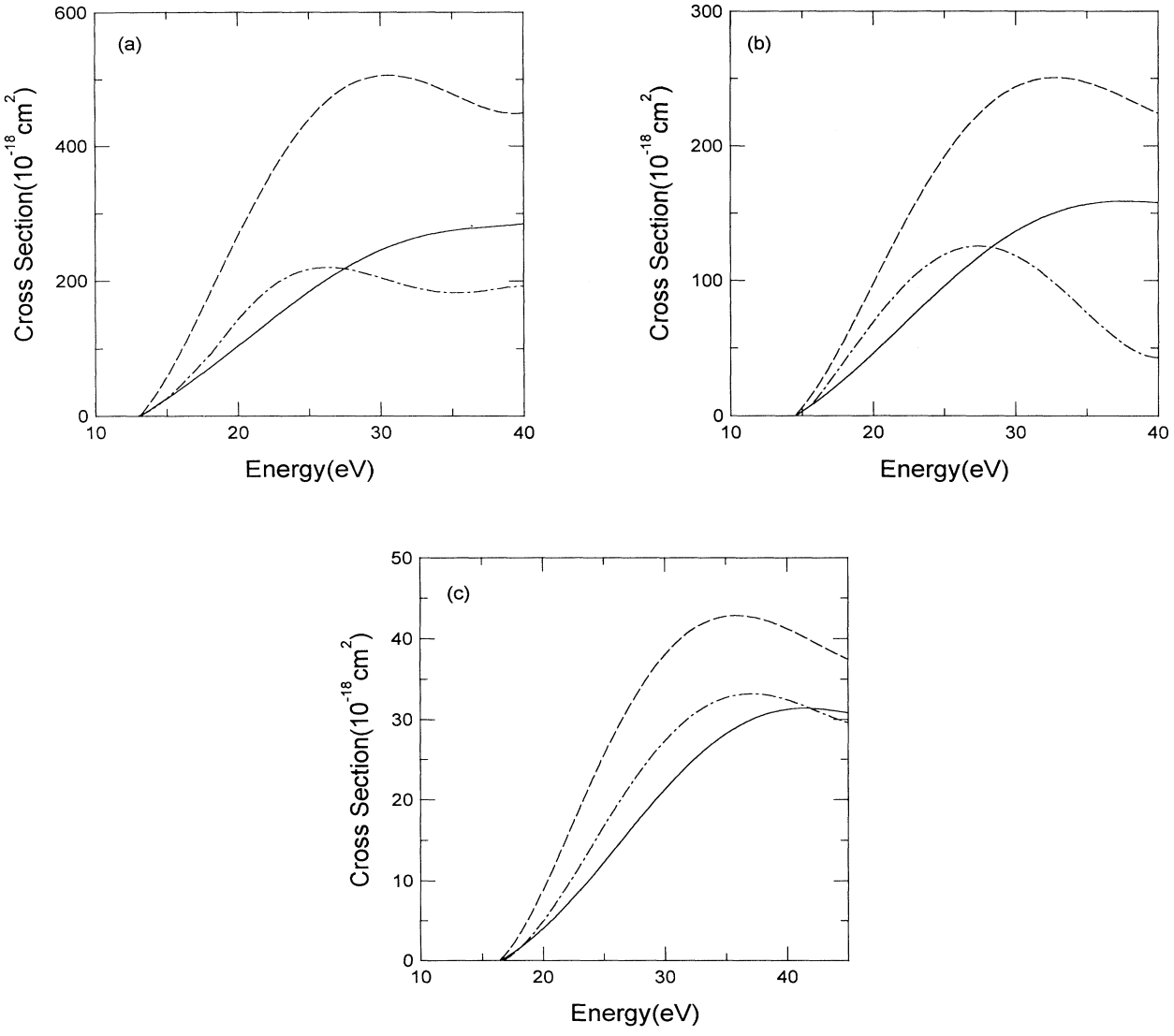

FIG. 10. Electron-impact ionization cross section for the (a) $3p^5\ ^2P \rightarrow 3p^4\ ^3P$, (b) $3p^5\ ^2P \rightarrow 3p^4\ ^1D$, and (c) $3p^5\ ^2P \rightarrow 3p^4\ ^1S$ transitions in Cl. Dashed curve, distorted-wave calculation with configuration-average continuum orbitals; Solid curve, distorted-wave calculation including both ground- and final-state correlations for the dipole-allowed excitation contribution; Chained curve, distorted-wave calculation including correlations and a polarization potential.

$$
\begin{aligned}
V(^3Pkd\ ^2D) &= V_{\rm CA}({\rm core}) + 4J^0_{3p} - \frac{1}{5}J^2_{3p} \\
&\quad + \frac{13}{15}K^1_{3p} - \frac{3}{35}K^3_{3p}\ , \\
V(^3Pkd\ ^2P) &= V_{\rm CA}({\rm core}) + 4J^0_{3p} + \frac{1}{5}J^2_{3p} \\
&\quad + \frac{9}{15}K^1_{3p} - \frac{9}{35}K^3_{3p}\ , \\
V(^1Dkd\ ^2D) &= V_{\rm CA}({\rm core}) + 4J^0_{3p} - \frac{1}{7}J^2_{3p} \\
&\quad + \frac{13}{15}K^1_{3p} - \frac{81}{245}K^3_{3p}\ , \\
V(^1Dkd\ ^2P) &= V_{\rm CA}({\rm core}) + 4J^0_{3p} - \frac{1}{5}J^2_{3p} \\
&\quad + \frac{9}{15}K^1_{3p} - \frac{9}{35}K^3_{3p}\ , \\
V(^1Dkd\ ^2S) &= V_{\rm CA}({\rm core}) + 4J^0_{3p} - \frac{2}{5}J^2_{3p} \\
&\quad + \frac{4}{15}K^1_{3p} - \frac{9}{35}K^3_{3p}\ , \\
V(^1Skd\ ^2D) &= V_{\rm CA}({\rm core}) + 4J^0_{3p} - \frac{2}{5}J^2_{3p} \\
&\quad + \frac{13}{15}K^1_{3p} - \frac{18}{35}K^3_{3p}\ . \qquad (5)
\end{aligned}
$$

Again the repulsive exchange terms in Eq. (5) cause a large reduction in the ionization cross sections. The third distorted-wave calculation includes the polarization potential of Eq. (3) (with $r_c = \bar{r}_{3p}$) in the scattering potential for all the continuum orbitals.

The effect of polarization in both Ar and Cl appears to be to shift the peak in the ionization cross section to lower energy. It is interesting to note that this same effect is also seen in the excitation cross section of Ar, when the polarization pseudostates are included in the calculation (see Fig. 7).

VI. CONCLUSIONS

We have presented the results of calculations of elastic and inelastic scattering from Ar and Cl, with a special emphasis on the effects of target polarization on the scattering cross sections. In the case of elastic scattering from Ar, comparisons with measurements and other calculations indicate that we have been able to achieve reasonable accuracy by performing R-matrix calculations for which the close-coupling expansions include those polarization pseudostates formed from dipole excitations out of the n=3 subshell. Because of the open $3p$ subshell, a similar calculation in Cl requires many more pseudostates in the close-coupling expansion, but should be of comparable accuracy. The polarization potential introduced by Baylis [25] with the $r_c \sim \bar{r}_{3p}$ is found to yield elastic cross sections in Ar which are in reasonably good agreement with the more extensive pseudostate calculations in the higher-energy region.

Our calculations of excitation to the lowest-lying metastable states in Ar and Cl are much more difficult than the elastic-scattering calculations. In addition to the real spectroscopic states that must be included in the close-coupling expansion, one must include a significant number of polarization pseudostates in order to represent the target polarization of the initial and final states. In Ar this required a total of 33 states, while in Cl, 51 states were needed. The effects of target polarization, especially in the final state, were found to be very large. This is particularly troublesome, since there are no indications that these calculations are converged, and many more states would have to be included for a complete description of polarization, even in the dipole approximation. In particular, one should include all pseudostates that can be reached via dipole excitations out of those spectroscopic states which couple strongly to either the initial or final state. However, since a calculation which included such additional pseudostates would be prohibitively large for the atoms considered here, we have not been able to investigate the significance of this added target polarization.

In our calculations, we solved for the polarization pseudo orbitals within a single-configuration framework, and then generated a configuration-interaction basis set of spectroscopic and pseudostates for use in the close-coupling calculation. On the other hand, Vo Ky Lan *et al.* [30] have generated polarization pseudostates within a multiconfiguration framework. In general, this should reduce the number of explicit pseudostates which must be included within the close-coupling expansion. As mentioned earlier, this was true in the case of elastic scattering from Ar by Bell *et al.* [8], where only a single ^1P pseudostate was required to represent the effects of polarization, instead of the four ^1P states included in our expansion. However, it is not at all clear that this multiconfiguration approach to polarization pseudostates would lead to a significant reduction in the number of required states for complex open-shell systems, where, in general, there are a large number of different LSΠ symmetries that must be represented by a unique set of radial spectroscopic and pseudo orbitals.

Thus, the use of polarization pseudostates, which has been shown to be quite successful for elastic scattering calculations, does not look promising for representing the effects of target polarization for electron-impact excitation of complex atoms. The sheer number of such states which must be included limits the applicability of this method. In the case of Ar and Cl, the fact that so many states were required just to represent excitation to the lowest lying excited states does not indicate that this method holds much promise for excitation to higher lying states, for which the number of required pseudostates would multiply significantly.

The use of a polarization potential to incorporate the effects of polarization within electron-impact excitation calculations has been quite successful for species with one electron above a closed subshell (for example, see Ref. [24]). However, we tried that approach in the case of Ar without any success. The difficulty arises from the fact that a single potential cannot properly represent the complex variation of the polarizability with atomic state. Thus, accurate excitation cross section calculations in complex atoms and low-charge-state ions, where target

polarization is important, remains a significant problem in atomic physics. It is clear that different approaches to the problem are called for.

We have also presented results for the ionization cross section of Ar and Cl, using a configuration-resolved distorted-wave method. Ground- and final-state correlations in the dipole-allowed excitation contributions to the total ionization cross section are shown to be important, reducing the cross section by more than a factor of two at its peak. Polarization, represented here using the polarization potential by Baylis with $r_c = \bar{r}_{3p}$, shifts the peaks in the cross sections to lower energies. However, it is not clear whether this improves agreement with experiment in Ar, and no comparisons are available in Cl. Until detailed comparisons with experiment are made, the accuracy obtained by using such potentials for ionization will be suspect.

ACKNOWLEDGMENTS

The first author wishes to thank D. Christian Griffin Jr. for his work on the workstation software and the graphics packages used in this project. We wish to thank V. M. Burke and C. J. Noble for providing us with a copy of the program FARM. This work was supported in part by the U.S. Department of Energy, Office of Fusion Energy, under Contract No. DE-FG05-93ER54218 with Rollins College and Contract No. DE-FG05-86-ER53217 with Auburn University; and by NATO under Contract No. CRG940134 with the University of Strathclyde.

[1] J. F. Williams, J. Phys. B **12**, 265 (1979).
[2] S. K. Srivastava, H. Tanaka, A. Chutjian, and S. Trajmar, Phys. Rev. A **23**, 2156 (1981).
[3] K. Jost, P. G. F. Bisling, F. Eschen, M. Felsmann, and L. Walther, in *Abstracts of the Thirteenth International Conference on the Physics of Electronic and Atomic Collisions, Berlin, 1983*, edited by J. Eichler, W. Fritsch, I. V. Hertel, N. Stolterfoht, and V. Willie (ICPEAC, Berlin, 1983), p. 91, and see Ref. [9].
[4] J. C. Nickel, K. Imre, D. F. Register, and S. Trajmar, J. Phys. B **18**, 125 (1985).
[5] J. Ferch, B. Granitza, C. Masche, and W. Raith, J. Phys. B **18**, 967 (1985).
[6] D. Andrick (unpublished), see Ref. [10].
[7] M. Ya. Amusia, N. A. Cherepkov, L. V. Chernysheva, D. M. Davidovic, and V. Radojevic, Phys. Rev. A **25**, 219 (1982).
[8] K. L. Bell, N. S. Scott, and M. A. Lennon, J. Phys. B **17**, 4757 (1984).
[9] Arati Dasgupta and A. K. Bhatia Phys. Rev. A **32**, 3335 (1985).
[10] H. P. Saha, Phys. Rev. A **43**, 4712 (1991).
[11] I. I. Fabrikant, J. Phys. B **27**, 4545 (1994).
[12] N. T. Padial, G. D. Meneses, F. J. da Paixao, Gy Csanak, and D C. Cartwright, Phys. Rev. A **23**, 2194 (1981).
[13] P. C. Ojha, P. G. Burke, and K. T. Taylor, J. Phys. B **15**, L507 (1982).
[14] R. C. Wetzel, F. A. Baiocchi, T. R. Hayes, and R. S. Freund, Phys. Rev. A **35**, 559 (1987).
[15] S. M. Younger, Phys. Rev. A **26**, 3177 (1982).
[16] K. Bartschat and P. G. Burke, J. Phys. B **21**, 2969 (1988).
[17] I. E. McCarthy and Y. Zhou, Phys. Rev. A **49**, 4597 (1994).
[18] K. A. Berrington, P. G. Burke, K. Butler, M. J. Seaton, P. J. Storey, K. T. Taylor, and Yu Yan, J. Phys. B **20**, 6379 (1987).
[19] V. M. Burke and C. J. Noble, Comput. Phys. Commun. (to be published).
[20] C. Froese Fischer, Comput. Phys. Commun. **64**, 369 (1991).
[21] A. Dalgarno and J. T. Lewis, Proc. R. Soc. London Sect. A **233**, 70 (1955).
[22] S. Huzinaga and C. Arnau, Phys. Rev. A **1**, 1285 (1970).
[23] D. W. Norcross and M. J. Seaton, J. Phys. B **9**, 2983 (1976).
[24] J. Mitroy, D. C. Griffin, D. W. Norcross, and M. S. Pindzola, Phys. Rev. A **38**, 3339 (1988).
[25] W. E. Baylis, J. Phys. B **10**, L583 (1977).
[26] Tomas Brage, Charlotte Froese Fischer, Nathalie Vaeck, Michael Godefroid, and Alan Hibbert, Phys. Scr. **48**, 533 (1993).
[27] M. S. Pindzola, D. C. Griffin, and C. Bottcher, J. Phys. B **16**, L355 (1983).
[28] T. M. Miller and B. Bederson, Adv. At. Mol. Phys. **13**, 1 (1977).
[29] A. Temkin, Phys. Rev. **107**, 1004 (1957).
[30] Vo Ky Lan, M. Le Dourneuf, and P. G. Burke, J. Phys. B **9**, 1065 (1976).
[31] J. J. Boyle, Phys. Rev. A **48**, 2860 (1993).
[32] T. N. Rescigno, Bull. Am. Phys. Soc. **39**, 1022 (1994), and (private communication).
[33] C. E. Moore, *Atomic Energy Levels*, Natl. Bur. Stand. (U.S.) Circ. No. 467 (U.S. GPO, Washington, DC, 1949), Vol. I.
[34] N. J. Mason and W. R. Newell, J. Phys. B **20**, 1357 (1987).
[35] A. Chutjian and D. C. Cartwright, Phys. Rev. A **23**, 2178 (1981).
[36] R. Scott Schappe, M. Bruce Schulman, L. W. Anderson, and Chun C. Lin, Phys. Rev. A **50**, 444 (1994).
[37] S. Bashkin and J. O. Stoner, *Atomic Energy Levels and Grotrian Diagrams* (North-Holland, Amsterdam, 1975), Vol. 3.
[38] N. S. Scott and A. Hibbert, Comput. Phys. Commun. **28**, 189 (1982).
[39] S. M. Younger, Phys. Rev. A **22**, 111 (1980).
[40] H. Jakubowicz and D. L. Moores, J. Phys. B **14**, 3733 (1981).
[41] M. E. Riley and D. G. Truhlar, J. Chem. Phys. **63**, 2182 (1975).
[42] M. Ya. Amusia, N. A. Cherepkov, and L. V. Chernysheva, Zh. Eksp. Teor. Fiz. **60**, 160 (1971) [Sov. Phys. JETP **33**, 90 (1971)].
[43] H. P. Kelly and R. L. Simons, Phys. Rev. Lett. **30**, 529 (1973).
[44] Z. D. Qian, S. L. Carter, and H. P. Kelly, Phys. Rev. A **33**, 1751 (1986).